Experimental evolution of bacterial survival on metallic copper

Feng Xu[1], Sha Liu[1], Naran Naren[1], Lily Li[1], Lvyan Ma[2], and Xue-Xian Zhang[1*]

[1]School of Natural Sciences, Massey University, Auckland 0745, New Zealand

[2]State Key Laboratory of Microbial Resources, Institute of Microbiology, Chinese Academy of Sciences, Beijing 100101, China

Running Title: Experimental evolution on copper

Keywords: metallic copper, brass, contact killing, biofilm, healthcare associated infections

Subject Category: Microbial Evolution

***Author for correspondence:** Xue-Xian Zhang

[1]School of Natural Sciences, Massey University at Albany, Auckland 0745, New Zealand

Phone: +64 (9) 2136593

E-mail: x.x.zhang1@massey.ac.nz

Abstract

Antimicrobial copper-containing surface materials have a great potential of reducing the risks of healthcare-associated infections (HAIs), but their increased use in hospital facilities may select copper resistant strains, causing concerns to antimicrobial resistance management. Here, we describe a long-term bacterial evolution experiment wherein a non-pathogenic strain of *Pseudomonas fluorescens* SBW25 was subjected to daily transfers in laboratory media with and without copper contact killing. The copper treatment sequentially involved two surface materials differing in Cu content and thus contact killing effectiveness: first on brass (Cu 63.5%) and then on pure copper (Cu 99.9%). A gradual increase in bacterial survival rate was observed over time on the related copper surfaces. For the final evolved populations after a total of 320 transfers, 37.8% cells of the copper evolved populations were able to survive 60 minutes on pure copper, whereas populations in the control lines remained sensitive under the same contact killing condition. Genome re-sequencing revealed ~540 mutations accumulated in the copper lines but only 71, on average, in the control lines (variant frequency > 0.5). The mutagenic activities of Cu^{+} ions were confirmed by measuring spontaneous mutation rate in a laboratory medium supplemented with copper sulphate at a non-inhibitory concentration. The copper evolved populations showed decreased production of biofilm, exoprotein, and pyoverdine; but they have evolved increased resistance to Cu^{+} ions and tobramycin (an aminoglycoside antibiotic). Together our data demonstrate the potential of bacteria to evolve prolonged survival on metallic copper, and implicate long-term impacts of increased copper usage in hospital environments.

Introduction

Copper in its ionic form (Cu^{2+} or Cu^{+}) is an essential micronutrient for almost all cellular organisms. It functions as a co-factor for oxidation-reduction reactions mediated by copper-containing oxidase, including those in the electron-transport chain. However, too much copper is harmful. This is largely due to its ability to produce hydroxyl radicals (OH^{-}) in a Fenton-like reaction. Cu^{+} ion toxicity is much higher for lower organisms such as bacteria and fungi, when compared with plants, animals, and humans (Ladomersky and Petris, 2015). When the toxicities of seventeen metals were compared with soil bacteria, copper ranks the fifth highest, behind silver, mercury, chromium, and cadmium (Drucker et al., 1979). Therefore, antimicrobial copper compounds have long been used in agriculture for the control of plant infectious diseases (La Torre et al., 2018; Lamichhane et al., 2018).

In recent years, however, the potential application of solid metallic copper (Cu) in public health has received increasing research attention. Healthcare-associated infections (HAIs) are a major health problem worldwide, affecting more than 10% patients admitted to hospitals for the treatments of other diseases (Weber et al., 2013). A major source of HAIs are microbial pathogens present on commonly touched items in hospitals (e.g., doorknobs, push plates, toilet seats, bed rails and IV poles), which are normally made of surface materials lacking any intrinsic antimicrobial properties (such as aluminium, stainless steel, plastics or woods). Therefore, introducing self-sanitizing surface materials like Cu and its alloys can potentially reduce the transmission of microbial pathogens via contacts between hospital patients, visitors, and healthcare workers. A wide range of microorganisms, including coronaviruses, can be killed within minutes of contact with a Cu surface [see reviews (Santo et al., 2008; Grass et al., 2011; Govind et al., 2021)]. The process is generally termed as Cu-mediated contact killing. Much attention has been focused on the roles of Cu in controlling various HAI-associated pathogens and its effectiveness in maintaining hospital environmental hygiene (Schmidt et al., 2012; Michels et al., 2015; Colin et al., 2018). The potential health risks remain largely unexplored (Santo et al., 2010; Maertens et al., 2021).

Cu products have been domestically used for centuries without any major health concerns, and thus, they are generally considered safe. The US Environmental Protection Agency has approved the registration of more than 500 types of Cu and its alloys as antimicrobial materials (Vincent et al., 2016). However, with an increased long-term use of Cu in hospital environment, pathogenic bacteria may develop Cu resistance, which is likely linked to microbial pathogenicity and antibiotic resistance (Virieux-Petit et al., 2022). Many field studies showed that copper amendment of agricultural soil selects for antibiotic resistant bacteria in the field (Berg et al., 2005; Knapp et al., 2011; Hu et al.,

2016). At the molecular level antibiotic resistance is linked to the cellular Cu^+ metabolism under the control of global regulators such as MarR as revealed in *E. coli* (Hao et al., 2014). More importantly, accumulation of toxic Cu^+ ions is a natural defence mechanism employed by human cells against bacterial infection (Hodgkinson and Petris, 2012; Chaturvedi and Henderson, 2014; Ladomersky and Petris, 2015). Therefore, in the worst-case scenario, Cu could select for highly virulent pathogenic bacteria with overlapping resistance to antibiotics, thus producing detrimental effects on the current antibiotic resistance management.

The mechanisms of Cu-mediated contact killing are not fully understood, but it has been generally accepted that toxic Cu^+ ions are the major cause of cell death (Vincent et al., 2018). Copper ions disrupt bacterial membrane integrity and further damage DNAs in the cytoplasm (Molteni et al., 2010; Hong et al., 2012; Warnes et al., 2012). However, the free Cu^{2+} ion concentrations on metallic Cu are not high enough to kill bacteria, and direct physical contact between bacteria and copper was shown to be crucial for the antimicrobial activities (Molteni et al., 2010; Mathews et al., 2013). Liu and Zhang (2016) proposed and experimentally tested a copper ion burst releasing (CIBR) model which posits that bacteria are rapidly killed by toxic Cu^+ ions continuously produced from chemical reactions between atomic copper and organic compounds in the bacterial cell surface structures, e.g., exopolysaccharides, lipopolysaccharides, and pili. According to the CIBR model, no bacteria would be able to survive from direct physical contact with a Cu surface, and it is only a matter of time how long it takes to be killed.

Bacterial cells have evolved three major types of mechanisms to survive in high copper environments: (1) copper efflux systems that act to pump excess Cu^+ ions outside of the cell; (2) sequestration systems that detoxify Cu^+ by specific high-affinity binding with proteins (e.g., copper chaperones); and (3) oxidation systems that convert Cu^+ into less toxic Cu^{2+} form (Giachino and Waldron, 2020). These systems collectively determine the adaptive capability of a bacterium to environmental stress imposed by ionic copper (Espirito Santo et al., 2008). However, as bacterial cells continuously absorb and accumulate more and more Cu^+ ions on metallic Cu surfaces, these resistance systems will eventually be outpaced, resulting in cell death. The only chance of survival is to escape Cu surfaces before being killed. This may occur in the hospital environments by means of human contacts. For example, oily substances from hands can physically separate bacteria from Cu surface and prevent further damage of the bacterial cell (de Carvalho and Caramujo, 2014).

Here, we hypothesis that optimization of the Cu^+ resistance determinants (and other yet-unknow genetic factors) can enhance bacterial survival on metallic copper, and selection can potentially occur

for mutants that survive longer on Cu surfaces. To test this hypothesis, we first performed a long-term evolution experiment by subjecting *Pseudomonas fluorescens* SBW25 to daily transfers in a laboratory medium with and without Cu contact killing. *P. fluorescens* SBW25 is a non-pathogenic model bacterium commonly used in experimental evolution (Zhang and Rainey, 2013). It belongs to the same genus as *P. aruginosa*, one of the most significant nosocomial pathogens (Moradali et al., 2017). Having observed an increase in bacterial survival rate on Cu surfaces, we subjected the evolved populations to genome re-sequencing, followed by characterization of phenotypes selected on the basis of the detected mutations. The data enable us to discuss the potential evolutionary impacts associated with an increased use of Cu-containing surface materials in hospitals for reducing the risks of HAIs.

Materials and Methods

Bacterial cultivation and evolution

P. fluorescens SBW25 and its naturally evolved derivatives were routinely cultured in lysogeny broth (LB) or King's B (KB) medium at 28ºC as previously described (Zhang and Rainey, 2013). When grown in the minimal M9 medium, glucose (0.4% or 22.2 mM) and NH_4Cl (1 mg/ml or 18.7 mM) were supplemented as the source of carbon and nitrogen, respectively. For biofilm assays, *P. fluoresces* was grown in the minimal M9 salt medium supplemented with succinate (20 mM) and histidine (10 mM) as the carbon and nitrogen sources. Tobramycin was purchased from Sigma-Aldrich and added at the indicated concentrations. Growth kinetics were determined in a microtiter plate using a Synergy 2 plate reader installed with Gen5 software (Bio-Tek Instruments). Strains were inoculated from cells stored at -80ºC freezer to ensure that bacteria in competition were physiologically equivalent (Zhang and Rainey, 2007a). Absorbance data were collected at 10-min intervals over a period of 24 hrs.

Experimental evolution was performed with SBW25-*lacZ*, which was derived from *P. fluorescens* SBW25 with the insertion of a promoterless *lacZ* gene at a neutral prophage site (Zhang and Rainey, 2007b). This strain forms distinctive blue colonies on LB agar plate supplemented with 5-bromo-4-chloro-3- indolyl-β-D-galactopyranoside (X-gal, 60 μg/ml). This property was used as a marker for detecting any potential contaminations. Strain identity was additionally checked by strain-specific PCR amplification of *xut* genes using primers xutA-compF and xutR-lacZF (Liu et al., 2015). As outlined in Figure 1, the work involved two treatments with and without Cu contact killing, and each was performed with eight independent evolutionary lines (Liu and Zhang, 2016). For Cu treatment,

cells from overnight culture were washed once with sterile water, and then 20 µl was dropped onto a Cu coupon (1 x 1 cm) placed in a Petri dish. After 60 min at room temperature, the brass coupon was transferred into a 30 ml plastic tube containing 2 ml LB medium. Survived cells on the coupon (~10,000) were released into the fresh medium by vigorous vortexing, and the coupon was subsequently removed with the help of a sterile inoculation loop. In the control line without Cu treatment, bacterial cultures were subjected to serial daily transfer by inoculating 5 µl culture into 5 ml fresh medium (thus, ten generations per transfer). The evolved bacterial populations were stored at -80°C freezer every 10 transfers for future assays of contact killing on Cu surfaces. The metal sheets of appropriately 1 mm thick were purchased from Wakefield Metals (Auckland, New Zealand): brass (UNS number C27200, 63.5 % Cu plus 36.5 % Zn), pure copper (UNS number C11000, 99.9 % Cu).

Copper resistance assays

Bacterial survival on Cu surfaces was measured using the so-called "wet" inoculation method (Molteni et al., 2010). Briefly, bacterial cells in overnight LB culture were spun down and re-suspended into the same amount of sterile water, and then 20 µl was inoculated onto the surface of a Cu coupon (1 x 1 cm). The coupons were placed beforehand in a Petri dish that contains a few drops of sterile water for keeping moisture. After a given period of treatment at room temperature (~20°C), bacteria on coupon were transferred into 2 ml H_2O in a 30 ml tube. Cells were released by vortexing, and colony formation units (cfu) were subsequently determined by dilution plating onto LB agar plates. Bacterial resistance to ionic copper was assessed in LB agar plate (or LB broth medium in 96-well microtiter plate) supplemented with varying concentrations of $CuSO_4$. The minimum inhibitory concentration (MIC) is defined as the lowest $CuSO_4$ concentration at which no colonies were observed after three days' incubation.

Biofilm quantification

The ability of *P. fluorescens* to form biofilm was quantitatively assessed using a standard method previously described by O'Toole (2011). Briefly, bacteria in an overnight culture were inoculated into a test medium by 100-times dilution, and then aliquoted into a 96-well microtiter plate (100 µl per well) placed in a 28°C static incubator for 1, 2 or 3 days. Biofilm formed on the inner wall of a well was stained with 125 µl of 0.1% Crystal Violet (CV) for 15 min. The dye was then dissolved using 125 µl of 30% acetic acid, and spectrophotometrically measured at the wavelength of 550 nm (A_{550}).

Bacteria fitness and mutation rate

Given that the evolved strains carry a neutral *lacZ* marker gene, their performance in laboratory medium was examined by direct competition with wild-type *P. fluorescens* SBW25. Competitive growth was initiated by mixing the two strains at a 1:1 ratio, and the mixed bacteria were inoculated into a fresh medium by 100-times dilution. The initial and final population densities (N_i) were determined at time $t = 0$ and at $t = T$ by dilution plating on LB + X-Gal plates. The average rate of population increase (i.e., Malthusian parameter m_i) is calculated for each strain using the formula of $m_i = \ln[N_i(T)/N_i(0)]$. Relative fitness is expressed here as the selection rate constant (SRC): $r_{ij} = m_i - m_j$, resulting in a fitness of zero when the two strains or populations are equally fit (Lenski, 1991).

Mutation rate was estimated using a modified procedure of fluctuation test as previously described (Pal et al., 2007). For each strain, six microcosms were set up and each was inoculated with ~500 cells. After grown in 6 ml LB broth for 24 hours in a shaken (160 rpm) incubator at 28^{o}C, final cell density and the frequency of antibiotics resistance mutant were counted by dilution plating in LB and LB + nalidixic acid (75 μg/ml) agar plates. Rate of spontaneous mutation was calculated using an integrated web tool named as bz-rates, which is based on Luria-Delbrück distribution-generating algorithm (Gillet-Markowska et al., 2015): www.lcqb.upmc.fr/bzrates.

Quantify pyoverdine and exoproteins

Pyoverdine production was quantified by measuring fluorescence of the supernatant at 460 nm with an excitation wavelength of 365 nm in a Synergy 2 multimode microplate reader (Bio-Tek Instruments). Data were expressed as relative fluorescence units (RFU) (Zhang and Rainey, 2013). Exoproteins were visualized by 12% sodium dodecyl sulfate-polyacrylamide gel electrophoresis (SDS-PAGE), wherein 20 μl cell-free supernatant prepared from overnight LB culture was loaded into each well. Protein concentration in the LB culture supernatant was estimated using the Quick Start^{TM} Braford Dye Reagent (Bio-Rad) following the manufacture's recommendation.

Genome sequencing and statistical analysis

Bacterial DNAs were prepared from the evolved populations using the Promega Wizard Genomic DNA purification Kit (In Vitro Technologies, Auckland). Sequencing was performed on an Illumina HiSeq 4000 platform using the services provided by Novogene Technology Co. Ltd (Beijing, China). Libraries were constructed from sheared DNA fragments of ~300 bp. The obtained 150 bp paired-end reads were processed in the Geneious 9.0.5 program (Biomatters Ltd, Auckland, New Zealand).

Sequences were mapped to the SBW25 reference genome (NC_012660.1) using the "Medium-Low Sensitivity/Fast" option. Mutations were identified by "Find Variations/SNPs" analysis with a "Minimum Variant Frequency" of 0.5 and default parameter settings for "Maximum Variant P-value" (10^{-6}), Minimum Strand-Bias *P*-value (10^{-5}), and "Find Polymorphism" (Inside & Outside CDS). Statistical analyses were performed using related tools available in GraphPad Prism v9.

Results

Experimental evolution led to an increase in bacterial resistance to metallic copper

As outlined in Fig. 1A, *P. fluorescens* SBW25 was subjected to daily transfer in 8 replicates, with and without Cu contact killing. The Cu treatment was first performed on brass and then shifted to pure copper after 200 transfers when the survival rate reached ~30% within a 60-min contact. Dynamic changes of copper resistance were assayed in parallel, using cells stored at -80°C freezer every 10 transfers. Results showed gradual increases of Cu resistance on the surfaces of brass and pure copper over the course of experimental evolution on Cu. For the final resultant 320th populations, an average of 37.8% cells can survive from contact killing on pure copper for 60 min. In contrast, cells in the eight control lines remained sensitive to metallic copper (Fig. 1).

Cu^+ ion toxicity is the major mechanism underlying the Cu-mediated contact killing. Thus, we hypothesised that the Cu evolved strains may have developed higher resistance to ionic copper. To test this, we first determined MIC of the final 320th populations on LB agar plates supplemented with varying concentrations of $CuSO_4$. Parallel to our expectation, the control lines and wild-type *P. fluorescence* SBW25 had the same MIC value of 3.25 mM, whereas the Cu evolved lines had an increased MIC value of 3.75 mM for 320D3 and 320D4, and 3.5 mM for the other six populations. Next, Cu^+ ion resistance was assessed in a 96-well microtiter plate containing 200 µl LB broth per well. The control lines (320C1 to 320C8) grew similarly as wild-type SBW25 in LB broth, and their growth was completely ceased with the supplementation of 3.5 mM $CuSO_4$ (data not shown). However, the Cu evolved populations showed significant growth with an average final cell density (A_{600}) of 0.39 in LB + $CuSO_4$ (3.5 mM) (Fig. 2B). Of note, a growth defect was observed for all Cu evolved populations when grown in LB broth without $CuSO_4$ supplementation (Fig. 2A). Together, our data indicate that the Cu evolved strains have achieved increased resistance to both metallic copper and ionic copper.

Genome re-sequencing of the evolved bacterial populations

To determine mutations accumulated over the course of experimental evolution, total DNAs were prepared from bacterial populations of the 320th and 200th transfers on copper (named 320D1 to 320D8 and 200D1 to 200D8, respectively). Additionally, final populations of the eight control lines (named 320C1 to 320C8) were also included in total DNA isolation and subsequent genome re-sequencing. Sequencing reads were aligned to the reference genome of *P. fluorescens* SBW25 (NC_012660.1) with ~99.5% pairwise identity. The average sequence depths were 81x for 320D1-D8, 165x for 200D1-D8, and 170x for 320C1-C8 populations. All mutations identified with a minimal variant frequency of 0.5 are listed in Supplementary Dataset 1. In the control lines, an average of 71 sequence variations were detected, and 21-24 mutations were fixed in the population (Table 1). Most variants are single nucleotide polymorphisms (SNPs, 75.7%). In contrast, about 540 variations were accumulated in the final copper-evolved populations (320D1 to 320D8), and the number of mutations fixed in the population (100%) ranges from 240 to 408. Even after 200 transfers the number of mutations in the Cu lines (130.6 on average) is significantly higher than that of the control lines (Fig. 3A). Together, the experimental evolution data implicate higher mutation rates associated with the Cu treatment.

Next, we tested the hypothesis that Cu exposure can enhance bacterial mutation rate as free Cu^{+} ions cause direct damage to DNAs. The mutation rates of *P. fluorescens* SBW25 were examined in LB medium with $CuSO_4$ being supplemented below the maximum non-inhibitory concentration. Results of the fluctuation test show that mutation rate was about 5-times greater when $CuSO_4$ (2 mM) was added into the LB broth (Fig, 3B). Additionally, it is interesting to note that mutations in DNA mismatch repairing systems were detected in both the copper evolved lines and the control line (Supplementary Dataset 1). Consequently, their spontaneous mutation rates were significantly higher than that of the wild-type SBW25 (Fig. S1).

Phenotypic characterization of the Cu evolved populations.

Mutations were detected in a total of 1392 open reading frames across the eight Cu evolved lines from 320D1 to 320D8. These genes can be classified into eight functional categories (Fig. 3A). While functional characterisation of these mutations was beyond the scope of this study, we used this information to investigate important phenotypes that are functionally relevant to copper homeostasis and general stress responses. Results are summarised below.

First, we examined their ability to form biofilms in comparison with the wild-type ancestor. Mutations were detected in fifty genes involved in the production of extracellular polymeric substances (EPS)

and the determination of cell envelop structure (Fig. 4A). These include the well-characterized *wss* genes and the associated *wsp* regulators for the synthesis of acetylated cellulose polymers; *algL* and *algK* for biosynthesis of alginate polymer (Supplementary Dataset 1). Of particular note are multiple unique mutations accumulated in three putative adhesin-encoding loci (Fig. 4B). Adhesins are a group of cell surface proteins that assist bacterial attachment to biotic and abiotic surfaces, and surface attachment is the crucial initial step of biofilm formation (Palmer et al., 2007). Together, all the genetic data suggest possible defects in biofilm formation. Indeed, biofilm formation was significantly lower for all eight Cu evolved populations when compared with wilt-type SBW25 in LB medium (Fig. 4C). The difference was much more pronounced when grown in the minimal M9 medium (Fig. 4D).

Next, we tested if there are any changes of proteins that are secreted into the laboratory medium, as mutations in exoprotein genes were clearly enriched during evolution on copper (Fig. 4A). Proteins in the supernatant of LB cultures were quantified using the Bradford method (Fig. S2A). Results showed that the amount of exoproteins was significantly lower in 320D6, 320D7 and 320D8 cultures when compared with the wild type, and cultures 320D1 to 320D5 were at the similar level as the negative control, i.e., the un-inoculated LB broth. Subsequent SDS-PAGE analysis detected a clear band for the wild-type strain, whereas the Cu evolved populations produced no visible bands (Fig. S2B).

Various nonsynonymous mutations were detected for pyoverdine synthesis genes in all eight Cu lines (Supplementary Dataset 1). These include five and seven unique mutations in *pvdI* and *pvdJ*, respectively, encoding the non-ribosomal peptide synthetase (NRPS) involved in the biosynthesis of the peptide backbone. Additionally, three unique *fpvA* mutations were fixed in three populations (320D2, 320D6, and 320D8). FpvA is an outer membrane ferric pyoverdine receptor, which regulates the expression of pyoverdine synthesis genes through the FpvA-FpvR-PvdS signalling pathway (Moon et al., 2008). To test the potential effects of these mutations, pyoverdine production was measured by growing bacteria in KB and LB broth media. Pyoverdine was pronouncedly produced in KB but not in LB as previously reported for SBW25 (Fig. S3). Pyoverdine production was almost abolished for 320D3 and 320D4 and occurred at significantly lower levels for other six populations in KB medium (Fig. S3A). Of note, pyoverdine was produced at significantly lower levels for the eight control lines in KB, despite the observation that no mutations of the previously identified pyoverdine genes were detected at a frequency larger than 50% (Fig. S3A). However, the control

lines produced pyoverdine at the similarly low levels as the wild type when grown in the LB broth medium (Fig. S3B).

Finally, we explored the potential effects on bacterial resistance to tobramycin, a commonly used antibiotic for treating *Pseudomonas* infections in humans (Yeung et al., 2011). Resistance was assayed in broth medium supplemented with varying concentrations of tobramycin. The assay was first performed in a minimal medium with succinate and histidine as the source of carbon and nitrogen, respectively. This is the nutrient condition that supports strong biofilm formation (Naren and Zhang, 2020), and the related catabolic genes have genetically been characterised (Naren and Zhang, 2021). As shown in Figure 5A, growth of the wild-type SBW25 was completely inhibited by tobramycin (2 μg/ml), while significant growth was detected for 320D1-D6. However, growth defects of varying degrees were detected in the same medium without antibiotic supplementation (Fig. 5A), and two populations (320D7 and 320D8) showed no growth within two days of incubation at 28ºC. This finding is not surprising because of mutations in DctB/DctD required for succinate utilization and CbrAB/NtrBC genes involved in the activation of histidine utilization (*hut*) genes. Additionally, mutations occurred in *hut* catabolic genes such as *hutI* and *hutT*$_h$ (Naren and Zhang, 2021). Next, we assayed tobramycin resistance in the nutrient-rich LB medium (Fig. 5C). All eight Cu evolved lines showed enhanced growth to varying extents when compared with wild type in the presence of tobramycin (2 μg/ml).

To examine the growth effects more closely, the evolved populations were subjected to direct competition with wild type in LB medium supplemented with and without tobramycin (2 μg/ml). A fitness zero indicates that the fitness of the tested population is identical to wild-type SBW25 (Fig. 5D). Results confirmed the finding that the Cu evolved populations exhibit reduced growth in LB medium (Fig. 2A) and their fitness were significantly less than zero ($P < 0.05$, Fig. 5D). In contrast, they were more fit than wild type in the presence of tobramycin (2 μg/ml) (Fig. 5D). Together, our data indicate that the Cu evolved populations displayed slower growth but higher tobramycin resistance phenotypes.

Discussion

In the present study we subjected a non-pathogenic model bacterium *P. fluorescens* SBW25 to daily transfers with and without a contact killing treatment on the surfaces of brass and pure copper. The experiment was designed to test the potential health concerns associated with the common use of antimicrobial Cu-containing surface materials for controlling hospital environmental hygiene, as a

new strategy for reducing the risks of HAIs. Results of this long-term evolution experiment demonstrate the evolutionary potentials of bacterial pathogens developing resistance to metallic Cu in terms of prolonged survival. Furthermore, we showed that the Cu evolved strains had increased resistance to Cu^{2+} ions when grown in laboratory media. This result is generally consistent with the established role of Cu^{2+} toxicity in Cu-mediated contact killings. Pathogens that can survive longer will clearly have a greater chance to escape Cu surfaces and persist in the hospital environments. Soil and oily substances on hands can protect bacteria from direct contact with Cu surfaces (Santo et al., 2010; de Carvalho and Caramujo, 2014). Therefore, our data suggest that natural selection may occur when Cu-containing surface materials are commonly used in hospital facilities, and proper regular cleaning is thus required to minimize the selection of resistant strains.

The antimicrobial efficacy of Cu surfaces is determined by many factors (Grass et al., 2011). In general, the antimicrobial activities of Cu alloys are proportional to the Cu content of the surface materials. For example, brass (Cu 63.5%) is less efficient than pure copper (Cu 99.9%). After 200 transfers ~70% cells were killed by contact killing on brass. However, when the same bacterial populations were subjected to contact killing on pure copper, more than 99.99% cells were killed (only 10,000 cells survived) under the similar condition (Fig. 1B). Apart from the material itself, environmental conditions such as temperature and moisture also produce significant influences on the efficacy of contact killing. It generally takes a shorter time for bacteria to be killed on dry surfaces relative to moist ones (Espirito Santo et al., 2011). The so-called “wet” inoculation method is commonly used in laboratory assays of bacterial contact killing, and it was adopted in this study in the process of experimental evolution. However, the moist surfaces may not reflect the complex situations in the healthcare environments.

Copper has long been used as a common coinage metal, including the New Zealand $1 coin made of copper, aluminium, and nickel (Cu 92%, Al 6%, Ni 2%). Thus, these coins have intrinsic antimicrobial activities, and bacteria were rapidly killed once inoculated onto their surfaces (Vriesekoop et al., 2016). In a previous study, Santo et al. (2010) conducted a microbiological survey of Cu alloy coins, and identified bacteria that are resistant against the toxic properties exerted by dry Cu surfaces. Most of these resistant isolates were Gram-positive staphylococci and micrococci, but also included Gram-negative species such as *Pseudomonas oleovorans* and *Pseudomonas putida*. Interestingly, these dry-surface-resistant strains seemingly had the similar levels of resistance to wet Cu surfaces and Cu^{+} ion resistance in laboratory medium, when compared with phylogenetically related reference strains (Santo et al., 2010). These data implicate the complexity of bacterial survival

on antimicrobial surfaces. The "sensitive" strains survived from contact killing due to soiling by organic matters (de Carvalho and Caramujo, 2014).

We showed that Cu^+ ions were mutagenic as we would expect based on their toxic effects on genomic DNAs (Warnes et al., 2012). Higher spontaneous mutation rates were observed even when $CuSO_4$ was added at a non-inhibitory concentration (Fig. 3B). This finding explains the significantly higher numbers of sequence variations observed in the Cu evolved lines relative to the non-Cu controls (Fig. 3A). However, no mutations were detected in the *cueAR* locus gene. This result is surprising because the *cueAR* operon is known to encode the primary Cu^+ efflux system in *P. fluorescence* SBW25 (Zhang and Rainey, 2007c, 2008). CueA is a copper-transporting P1-type ATPase whose expression is induced by copper under the control of a MerR-type transcriptional activator CueR. In addition to *cueA*, CueR regulates the expression of many other genes involved in copper homeostasis. These include *cueZ* (*pflu0660*) encoding a copper chaperone of 65 amino acids in length. Only one *cueZ* mutation (C56T) was detected in one of the eight Cu evolved lines, and this mutation was not fixed in the population 320D6. However, mutations were detected in the chromosome-encoded CopRS two-component system in seven out of the eight Cu evolved populations (*pflu1575* and *flu1576*, Supplementary Dataset 1). Interestingly, deletion of *copS* gene resulted in an increased resistance to Cu^+ (Zhang and Rainey, 2008). Thus, the new evolution data support the previous conclusion that the CopRS-regulated genes (specifically, *copC* and *copD*) act as a Cu^+ uptake system, and their loss of function would benefit bacterial survival in high Cu environments.

The Cu evolved populations have severe growth defects in LB broth medium. This strongly suggests that selection was dominated by adaptation to copper stress rather than growth enhancement in the laboratory medium. Many mutations occurred in catabolic genes (31.75%, 442/1392) and their regulators (Table S2). These include two two-component systems CbrAB and NtrBC, which play global regulatory roles in cellular carbon and nitrogen metabolisms (Naren and Zhang, 2021). Both CbrAB and NtrBC are involved in the regulation of bacterial growth in biofilms for *Pseudomonas* (Amador et al., 2016; Alford et al., 2020). The CbrA kinase is functionally linked to antibiotic resistance. Inactivation of *cbrA* gene in *P. aeruginosa* PA14 caused an increase of tobramycin minimal inhibitory concentration (MIC) from 2 μg/ml for wild type to 8 μg/ml for the Δ*cbrA* mutant (Yeung et al., 2011). These mutations thus partially explain the observed phenotypes with regard to a decrease of biofilm formation but an increased resistance to tobramycin.

All eight replicate populations in the Cu evolution line carried a mutation in *mutL gene*, which encodes a DNA mismatch repair protein. Inactivation of *mutL* is known to produce a mutator

phenotype with a higher spontaneous mutant rate (Matic, 2019). The specific *mutL* mutation involved one guanine deletion at a position that contains five guanine residues (1174_G5 to 1174_G4). Thus, this is likely a mutational hotspot. The same mutation was detected but not fixed in the 200th populations (200D1 - 200D8). However, among the 320th populations, this particular *mutL* mutation was fixed in three out of the eight populations (320D1, 320D6, and 320D7). An additional new *mutL* mutation (T875C) was found in population 320D5. This finding suggests that higher mutation rate is advantageous for bacterial adaptation to Cu stress. Finally, we noted that the same mutations were found in multiple replicate lines which cannot be explained simply by parallel evolution due to their high frequencies of occurrence. In this work we used a *lacZ* marker to detect potential contamination by other bacteria from the environments. However, strains in each replicate line were not individually barcoded; and consequently, we are unable to exclude the possibility of cross-line contaminations. This may affect the absolute independence of the eight replicates within a treatment, but not the significant differences between Cu-treated and Cu-untreated control lines.

In conclusion, the experimental evolution data presented here show that bacteria were capable of evolving prolonged survival on the surfaces of metallic copper. A significantly higher number of mutations (540 on average) were accumulated in the final copper-evolved lines relative to an average of 71 mutations found in the control lines. The resulting resistant strains showed increased resistance to Cu^+ ions, but no mutations were detected in the previously identified Cu^+-efflux system CueA and its regulator CueR. Thus, *Pseudomonas* must possess some yet-unknown mechanisms that act to maintain cellular copper homeostasis. Genes in the CopRS regulon are the likely candidates for further characterization. With regard to phenotypic changes, the Cu evolved strains showed decreased abilities to grow in laboratory media, biofilm formation, pyoverdine production, and exoprotein secretion; but more importantly, they have evolved increased resistance to tobramycin. Together, our data suggest that the long-term evolutionary impacts should be considered if copper were to become commonly used in the hospital environments.

ACKNOWLEDGEMENTS

We thank Stephen Ritchie and Tim Cooper for helpful discussions. This work was financially supported by the Maurice and Phyllis Paykel Trust (MPPT) and the New Zealand MBIE Catalyst Fund (project number 92846082). F. Xu acknowledges support of an international visitor's scholarship from Nanchang University.

REFERTENCES

Alford, M.A., Baghela, A., Yeung, A.T.Y., Pletzer, D., and Hancock, R.E.W. (2020) NtrBC Regulates Invasiveness and Virulence of *Pseudomonas aeruginosa* During High-Density Infection. *Front Microbiol* **11**: 773.

Amador, C.I., Lopez-Sanchez, A., Govantes, F., Santero, E., and Canosa, I. (2016) A *Pseudomonas putida cbrB* transposon insertion mutant displays a biofilm hyperproducing phenotype that is resistant to dispersal. *Environ Microbiol Rep* **8**: 622-629.

Berg, J., Tom-Petersen, A., and Nybroe, O. (2005) Copper amendment of agricultural soil selects for bacterial antibiotic resistance in the field. *Letters in Applied Microbiology* **40**: 146-151.

Chaturvedi, K.S., and Henderson, J.P. (2014) Pathogenic adaptations to host-derived antibacterial copper. *Frontiers in Cellular and Infection Microbiology* **4**: 1-12.

Colin, M., Klingelschmitt, F., Charpentier, E., Josse, J., Kanagaratnam, L., De Champs, C., and Gangloff, S.C. (2018) Copper Alloy Touch Surfaces in Healthcare Facilities: An Effective Solution to Prevent Bacterial Spreading. *Materials* **11**: 2479.

de Carvalho, C.C.C.R., and Caramujo, M.J. (2014) Bacterial diversity assessed by cultivation-based techniques shows predominance of *Staphylococccus* species on coins collected in Lisbon and Casablanca. *FEMS Microbiology Ecology* **88**: 26-37.

Drucker, H., Garland, T.R., and Wildung, R.E. (1979) Metabolic response of microbiota to chromium and other metals. In *Trace metals in health and disease*. Kharasch, N. (ed). New York: Raven Press, pp. 1-25.

Espirito Santo, C., Taudte, N., Nies, D.H., and Grass, G. (2008) Contribution of copper ion resistance to survival of Escherichia coli on metallic copper surfaces. *Appl Environ Microbiol* **74**: 977-986.

Espirito Santo, C., Lam, E.W., Elowsky, C.G., Quaranta, D., Domaille, D.W., Chang, C.J., and Grass, G. (2011) Bacterial killing by dry metallic copper surfaces. *Appl Environ Microbiol* **77**: 794-802.

Giachino, A., and Waldron, K.J. (2020) Copper tolerance in bacteria requires the activation of multiple accessory pathways. *Mol Microbiol* **114**: 377-390.

Gillet-Markowska, A., Louvel, G., and Fischer, G. (2015) bz-rates: A Web Tool to Estimate Mutation Rates from Fluctuation Analysis. *G3 (Bethesda)* **5**: 2323-2327.

Govind, V., Bharadwaj, S., Ganesh, M.R.S., Vishnu, J., Shankar, K.V., Shankar, B., and Rajesh, R. (2021) Antiviral properties of copper and its alloys to inactivate covid-19 virus: a review. *Biometals* **34**: 1217-1235.

Grass, G., Rensing, C., and Solioz, M. (2011) Metallic Copper as an Antimicrobial Surface. *Applied and Environmental Microbiology* **77**: 1541-1547.

Hao, Z.Y., Lou, H.B., Zhu, R.F., Zhu, J.H., Zhang, D.M., Zhao, B.X.S. et al. (2014) The multiple antibiotic resistance regulator MarR is a copper sensor in *Escherichia coli*. *Nature Chemical Biology* **10**: 21-U48.

Hodgkinson, V., and Petris, M.J. (2012) Copper Homeostasis at the Host-Pathogen Interface. *Journal of Biological Chemistry* **287**: 13549-13555.

Hong, R., Kang, T.Y., Michels, C.A., and Gadura, N. (2012) Membrane lipid peroxidation in copper alloy-mediated contact killing of Escherichia coli. *Appl Environ Microbiol* **78**: 1776-1784.

Hu, H.W., Wang, J.T., Li, J., Li, J.J., Ma, Y.B., Chen, D.L., and He, J.Z. (2016) Field-based evidence for copper contamination induced changes of antibiotic resistance in agricultural soils. *Environmental Microbiology* **18**: 3896-3909.

Knapp, C.W., McCluskey, S.M., Singh, B.K., Campbell, C.D., Hudson, G., and Graham, D.W. (2011) Antibiotic Resistance Gene Abundances Correlate with Metal and Geochemical Conditions in Archived Scottish Soils. *Plos One* **6**.

La Torre, A., Iovino, V., and Caradonia, F. (2018) Copper in plant protection: current situation and prospects. *Phytopathologia Mediterranea* **57**: 201-236.

Ladomersky, E., and Petris, M.J. (2015) Copper tolerance and virulence in bacteria. *Metallomics* **7**: 957-964.

Lamichhane, J.R., Osdaghi, E., Behlau, F., Kohl, J., Jones, J.B., and Aubertot, J.N. (2018) Thirteen decades of antimicrobial copper compounds applied in agriculture. A review. *Agronomy for Sustainable Development* **38**.

Lenski, R.E. (1991) Quantifying fitness and gene stability in microorganisms. *Biotechnology* **15**: 173-192.

Liu, S., and Zhang, X.X. (2016) Small colony variants are more susceptible to copper-mediated contact killing for *Pseudomonas aeruginosa* and *Staphylococcus aureus*. *Journal of Medical Microbiology* **65**: 1143-1151.

Liu, Y., Rainey, P.B., and Zhang, X.X. (2015) Molecular mechanisms of xylose utilization by *Pseudomonas fluorescens*: overlapping genetic responses to xylose, xylulose, ribose and mannitol. *Mol Microbiol* **98**: 553-570.

Maertens, L., Matroule, J.Y., and Van Houdt, R. (2021) Characteristics of the copper-induced viable-but-non-culturable state in bacteria. *World Journal of Microbiology & Biotechnology* **37**.

Mathews, S., Hans, M., Mucklich, F., and Solioz, M. (2013) Contact Killing of Bacteria on Copper Is Suppressed if Bacterial-Metal Contact Is Prevented and Is Induced on Iron by Copper Ions. *Applied and Environmental Microbiology* **79**: 2605-2611.

Matic, I. (2019) Mutation Rate Heterogeneity Increases Odds of Survival in Unpredictable Environments. *Mol Cell* **75**: 421-425.

Michels, H.T., Keevil, C.W., Salgado, C.D., and Schmidt, M.G. (2015) From Laboratory Research to a Clinical Trial: Copper Alloy Surfaces Kill Bacteria and Reduce Hospital-Acquired Infections. *Herd-Health Environments Research & Design Journal* **9**: 64-79.

Molteni, C., Abicht, H.K., and Solioz, M. (2010) Killing of Bacteria by Copper Surfaces Involves Dissolved Copper. *Applied and Environmental Microbiology* **76**: 4099-4101.

Moon, C.D., Zhang, X.X., Matthijs, S., Schafer, M., Budzikiewicz, H., and Rainey, P.B. (2008) Genomic, genetic and structural analysis of pyoverdine-mediated iron acquisition in the plant growth-promoting bacterium *Pseudomonas fluorescens* SBW25. *BMC Microbiol* **8**: 7.

Moradali, M.F., Ghods, S., and Rehm, B.H. (2017) Pseudomonas aeruginosa Lifestyle: A Paradigm for Adaptation, Survival, and Persistence. *Front Cell Infect Microbiol* **7**: 39.

Naren, N., and Zhang, X.X. (2020) Global Regulatory Roles of the Histidine-Responsive Transcriptional Repressor HutC in Pseudomonas fluorescens SBW25. *J Bacteriol* **202**.

Naren, N., and Zhang, X.X. (2021) Role of a local transcription factor in governing cellular carbon/nitrogen homeostasis in *Pseudomonas fluorescens*. *Nucleic Acids Res* **49**: 3204-3216.

O'Toole, G.A. (2011) Microtiter dish biofilm formation assay. *Journal of Visualized Experiments*.

Pal, C., Macia, M.D., Oliver, A., Schachar, I., and Buckling, A. (2007) Coevolution with viruses drives the evolution of bacterial mutation rates. *Nature* **450**: 1079-1081.

Palmer, J., Flint, S., and Brooks, J. (2007) Bacterial cell attachment, the beginning of a biofilm. *J Ind Microbiol Biotechnol* **34**: 577-588.

Santo, C.E., Morais, P.V., and Grass, G. (2010) Isolation and Characterization of Bacteria Resistant to Metallic Copper Surfaces. *Applied and Environmental Microbiology* **76**: 1341-1348.

Santo, C.E., Taudte, N., Nies, D.H., and Grass, G. (2008) Contribution of copper ion resistance to survival of *Escherichia coli* on metallic copper surfaces. *Applied and Environmental Microbiology* **74**: 977-986.

Schmidt, M.G., Attaway, H.H., Sharpe, P.A., John, J., Sepkowitz, K.A., Morgan, A. et al. (2012) Sustained Reduction of Microbial Burden on Common Hospital Surfaces through Introduction of Copper. *Journal of Clinical Microbiology* **50**: 2217-2223.

Vincent, M., Hartemann, P., and Engels-Deutsch, M. (2016) Antimicrobial applications of copper. *Int J Hyg Environ Health* **219**: 585-591.

Vincent, M., Duval, R.E., Hartemann, P., and Engels-Deutsch, M. (2018) Contact killing and antimicrobial properties of copper. *Journal of Applied Microbiology* **124**: 1032-1046.

Virieux-Petit, M., Hammer-Dedet, F., Aujoulat, F., Jumas-Bilak, E., and Romano-Bertrand, S. (2022) From Copper Tolerance to Resistance in Pseudomonas aeruginosa towards Patho-Adaptation and Hospital Success. *Genes* **13**.

Vriesekoop, F., Chen, J., Oldaker, J., Besnard, F., Smith, R., Leversha, W. et al. (2016) Dirty Money: A Matter of Bacterial Survival, Adherence, and Toxicity. *Microorganisms* **4**.

Warnes, S.L., Caves, V., and Keevil, C.W. (2012) Mechanism of copper surface toxicity in *Escherichia coli* O157:H7 and *Salmonella* involves immediate membrane depolarization followed by slower rate of DNA destruction which differs from that observed for Gram-positive bacteria. *Environmental Microbiology* **14**: 1730-1743.

Weber, D.J., Anderson, D., and Rutala, W.A. (2013) The role of the surface environment in healthcare-associated infections. *Current Opinion in Infectious Diseases* **26**: 338-344.

Yeung, A.T.Y., Bains, M., and Hancock, R.E.W. (2011) The Sensor Kinase CbrA Is a Global Regulator That Modulates Metabolism, Virulence, and Antibiotic Resistance in Pseudomonas aeruginosa. *Journal of Bacteriology* **193**: 918-931.

Zhang, X.X., and Rainey, P.B. (2007a) Genetic analysis of the histidine utilization (*hut*) genes in *Pseudomonas fluorescens* SBW25. *Genetics* **176**: 2165-2176.

Zhang, X.X., and Rainey, P.B. (2007b) Construction and validation of a neutrally-marked strain of *Pseudomonas fluorescens* SBW25. *J Microbiol Methods* **71**: 78-81.

Zhang, X.X., and Rainey, P.B. (2007c) The role of a P1-type ATPase from *Pseudomonas fluorescens* SBW25 in copper homeostasis and plant colonization. *Mol Plant Microbe Interact* **20**: 581-588.

Zhang, X.X., and Rainey, P.B. (2008) Regulation of copper homeostasis in *Pseudomonas fluorescens* SBW25. *Environ Microbiol* **10**: 3284-3294.

Zhang, X.X., and Rainey, P.B. (2013) Exploring the sociobiology of pyoverdin-producing *Pseudomonas*. *Evolution* **67**: 3161-3174.

Table 1. Number of mutations occurred at frequencies larger than 50% in a population

Population*	Total	Indel	SNPs	Transversion	Transition	Mutation (100%)
320C1	59	15	44	2	42	23
320C2	67	18	49	2	47	23
320C3	89	21	68	4	64	24
320C4	75	19	56	4	52	21
320C5	69	16	53	3	50	24
320C6	67	16	51	3	48	21
320C7	77	17	60	3	57	23
320C8	66	16	50	3	47	21
200D1	124	22	102	2	100	14
200D2	126	22	104	3	101	22
200D3	135	25	110	2	108	16
200D4	160	26	134	1	133	23
200D5	126	23	103	2	101	21
200D6	126	23	103	2	101	8
200D7	118	19	99	2	97	31
200D8	130	31	99	1	98	9
320D1	530	83	447	11	436	240
320D2	547	98	449	15	434	313
320D3	501	83	418	12	406	238
320D4	577	92	485	14	471	301
320D5	460	80	380	14	366	206
320D6	483	88	395	15	380	211
320D7	593	106	487	26	461	399
320D8	630	102	528	28	500	408

*Populations named 320C1 to 320C8 are the control lines after 320 transfers in LB broth. Populations evolved on copper after 200 and 320 transfers are designated 200D1 to 200D8 and 320D1 to 320D8, respectively.

Table S1. List of two-component regulatory systems with mutations occurred during experimental evolution on copper

Locus tag	Gene	Function	Variation
Pflu0182		RR	C708T
Pflu0286	*dctD*	RR, succinate uptake	T38C,
Pflu0287	*dctB*	RR, succinate uptake	A21G, A206G
Pflu0344	*glnL/ntrB*	RR, cellular nitrogen regulator	A206G
Pflu0610		Hybrid TCS	A23G
Pflu0637		SK	C143T
Pflu0700		SK	T1052C, A623G
Pflu1132		RR	A337G
Pflu1135		SK	C736T
Pflu1451	*tctD*	RR, tricarboxylic acids uptake, biofilm formation	T207C
Pflu1575	*copS*	SK, copper homeostasis	C555CC insertion
Pflu1576	*copR*	RR, copper homeostasis	T155C
Pflu1679	*kdpD*	SK, potassium homeostasis	A369G, A1359G
Pflu1680	*kdpE*	RR, potassium homeostasis	C123T
Pflu1837		Hybrid TCS	C560T
Pflu1849		SK	G115GG insertion
Pflu2122		SK	C1165T
Pflu2181		Hybrid TCS	G3318GG insertion
Pflu2249		Hybrid TCS	C1083T
Pflu2267		Hybrid TCS	T800C, G22265GG insertion
Pflu2337		SK	C801T
Pflu2515		SK	C1045T
Pflu2571		SK	C345T
Pflu2572		RR	C545T
Pflu2626		Hybrid TCS	C562T
Pflu2723		SK	C327T
Pflu2939		SK	C547T
Pflu3023		Hybrid TCS	A346G, G663A
Pflu3074		RR	G549A
Pflu3075		SK	T812C
Pflu3447		SK	A66G, T849C

Pflu3555		SK	G974A
Pflu3654		SK	T434C
Pflu4121	*baeS*	SK, multidrug resistance	T599C, G306A
Pflu4122	*baeR*	RR, multidrug resistance	T254C
Pfl4171		RR	C279T
Pflu4172		SK	T223C, G760A
Pflu4404		RR	T401C
Pflu4432		Hybrid TCS	T1294C
Pflu4441		RR	C172T
Pflu4443	*fleQ*	RR, a master regulator of cell motility	G322GG insertion, T1352C
Pflu4471		Hybrid TCS	G2483A
Pflu4723		SK	T1595C
Pflu4724		RR	C109T
Pflu4884		RR	T392C
Pflu4929		SK	G1125A
Pflu4953		SK	G873A
Pflu4983		SK	G660A
Pflu4984		RR	T407C
Pflu5118		RR	T300C
Pflu5236	*cbrA*	SK, cellular carbon metabolism	G1087A
Pflu5237	*cbrB*	RR, cellular carbon metabolism	A656G
Pflu5398		Hybrid TCS	C190T, T1577C
Pflu5640	*creC*	SK, carbon source responsive, biofilm formation, antibiotic resistance	A349G, G1377A

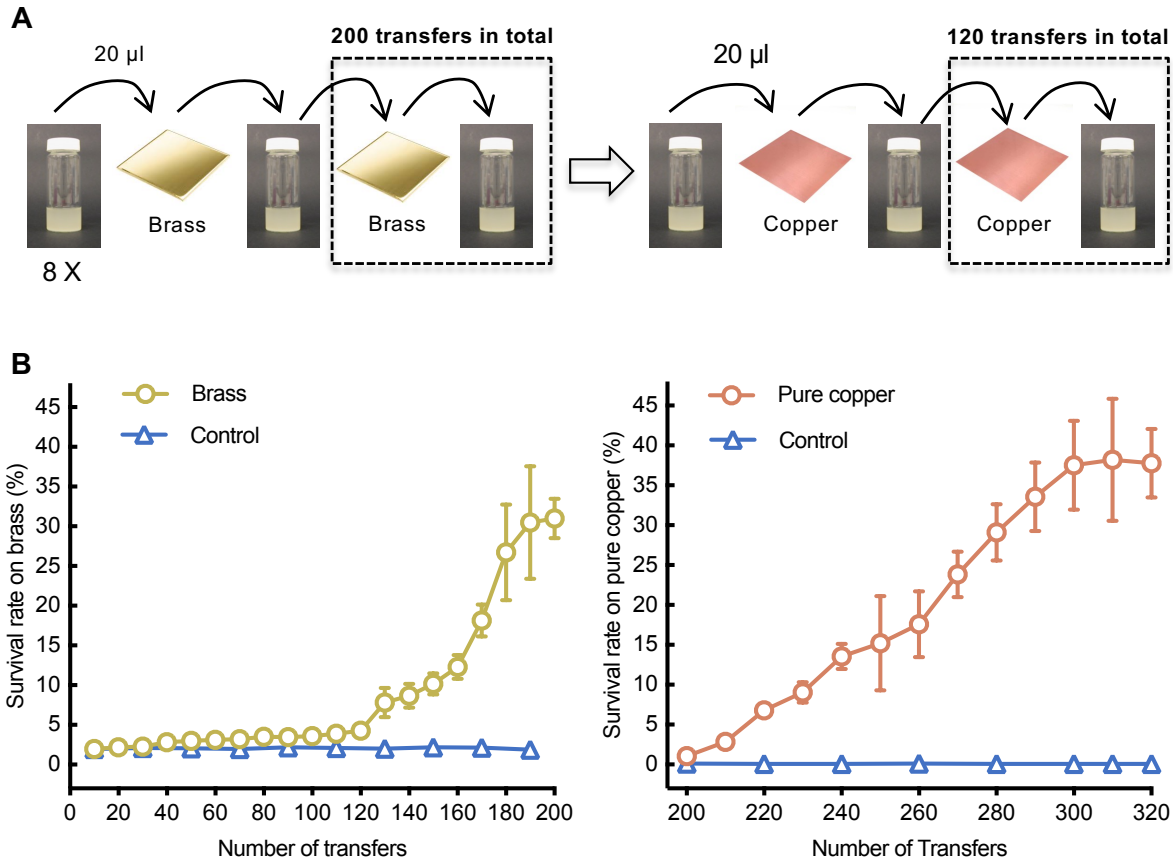

Figure 1. Increase in bacterial survival on solid Cu surfaces during experimental evolution.

(A) An outline of the experimental procedures. Bacteria grown in 2 ml LB broth in eight replicates were subjected to bottleneck every 24 hrs with Cu treatment. For each transfer, 20 µl of washed cells from overnight culture were inoculated onto the surface of a metal coupon. After 60 minutes at room temperature, cells on the coupon were suspended into a fresh LB broth. Cells survived from the contact killing would form a new population for the next round of contact killing. The Cu material was shifted from bass to pure copper when the maximum survival rates were reached after 200 transfers. Bacteria in the eight control lines were propagated by normal daily transfers without Cu treatment (not shown in the schematic map).

(B) Rates of bacterial contact-killing on the surfaces of brass (left) and pure copper (right). The evolved populations were stored in -80°C freezer at every 10 transfers, and their resistance levels were determined in parallel on the brass and copper surfaces. Data are means and standard errors of 8 replicate cultures for each evolutionary line.

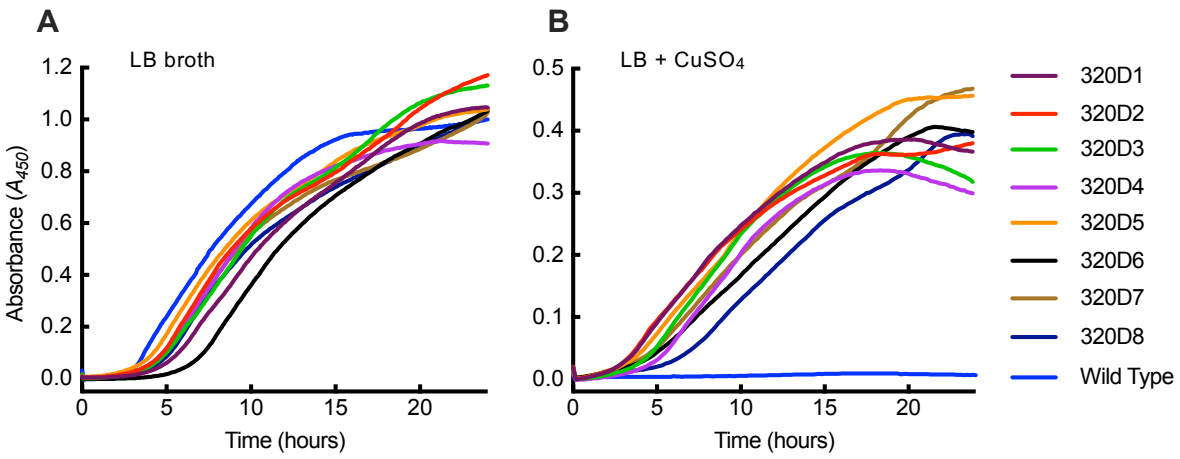

Figure 2. The Cu-evolved *Pseudomonas* populations showed an increase in Cu^{+} resistance.

Growth kinetics were measured with bacteria grown in 96-well microtiter plate in LB broth **(A)** and LB broth supplemented with 3.5 mM $CuSO_4$ **(B)**. Absorbance at the wavelength of 450 nm (A_{450}) was recorded every 10 minutes after inoculation. Data are means of five independent cultures (standard errors are small and not shown for clarity).

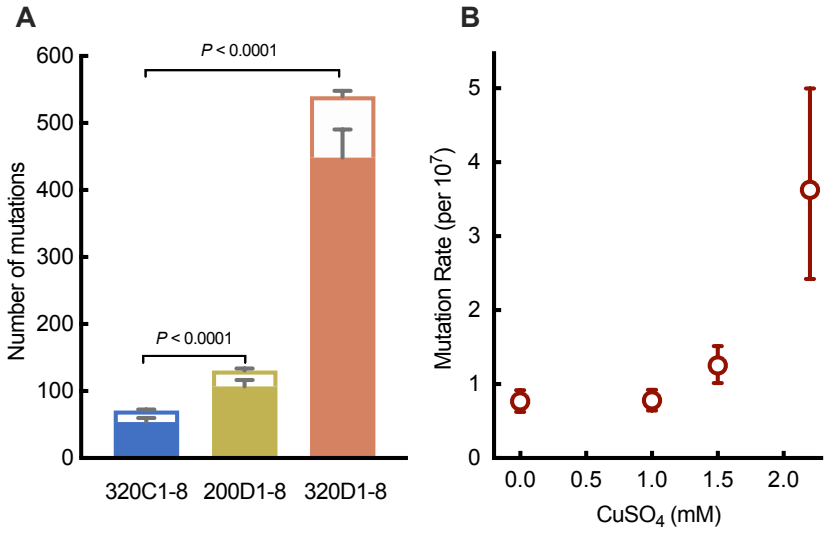

Figure 3. Higher mutation rates induced by solid Cu and Cu^{2+} ions.

(A) Total number of mutations accumulated in the control lines after 320 transfer (320C1 - 320C8) and the Cu treatment lines after 200 transfers (200D1 - 200D8) and 320 transfer (320D1 - 320D8). The number of indel mutations (open bars) is stacked on top of SNPs (solid bars). Data are means and 95% CI of eight replicate lines.

(B) Mutation rates estimated by fluctuation test in LB broth supplemented with varying concentrations of copper sulphate. Data are means and 95% CI of eight independent cultures calculated using the *bz-rates* Web tool.

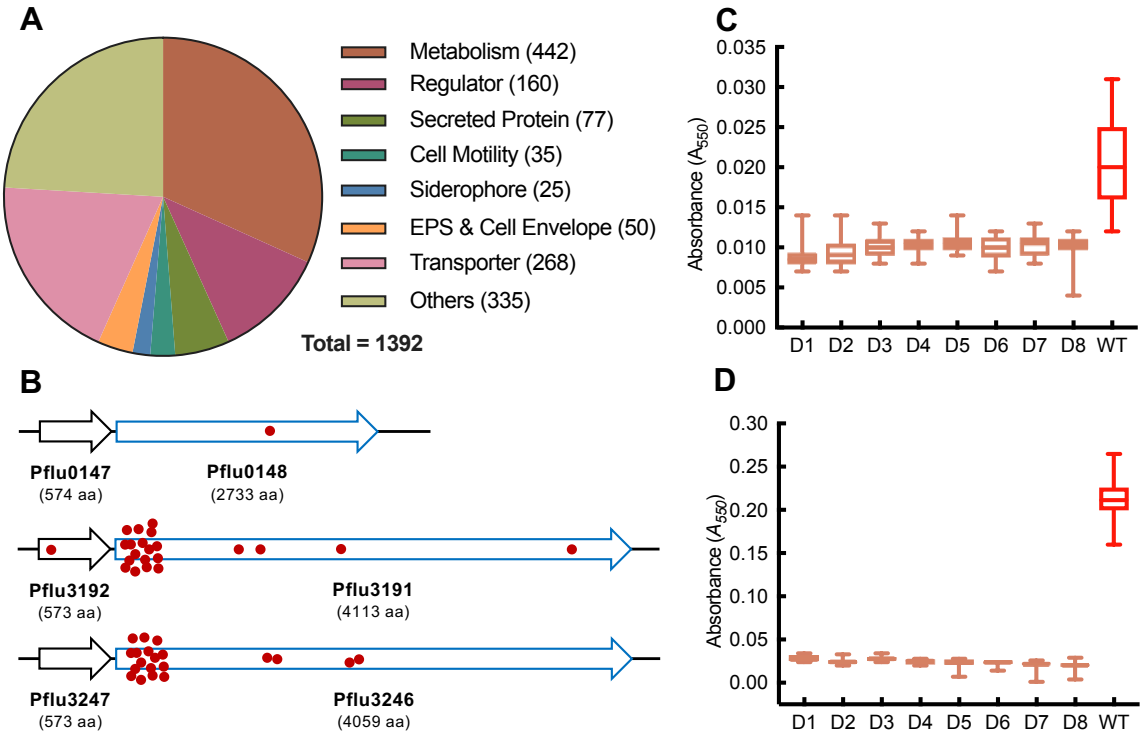

Figure 4. A functional overview of gene mutations and the phenotypic effects on biofilm formation.

(A) Functional distribution of mutated genes in the eight copper evolution lines. **(B)** Schematic maps of three adhesion-encoding loci. Red dots denote the approximate positions of the observed mutations. **(C)** Biofilm formation in LB medium. **(D)** Biofilm formation in minimal M9 medium with glucose and NH_4Cl. Biofilms on the inner surfaces of a 96-well microtiter plate were stained with 0.1% crystal violet (CV) and the dye was then solubilized with 30% acetic acid, followed by measurement of absorbance at the wavelength of 550 nm (A_{550}). The line in the middle of the box represents the median of 10 independent cultures, whereas the bottom and top boxes represent the 25th and 75th percentiles, respectively. The lower and upper whiskers indicate the smallest and largest values, respectively. One-way ANOVA multiple comparisons indicate significant differences ($P < 0.05$) with the related wild-type (WT) controls. D1 to D8 represents the 320th populations 320D1 to 320D8, respectively.

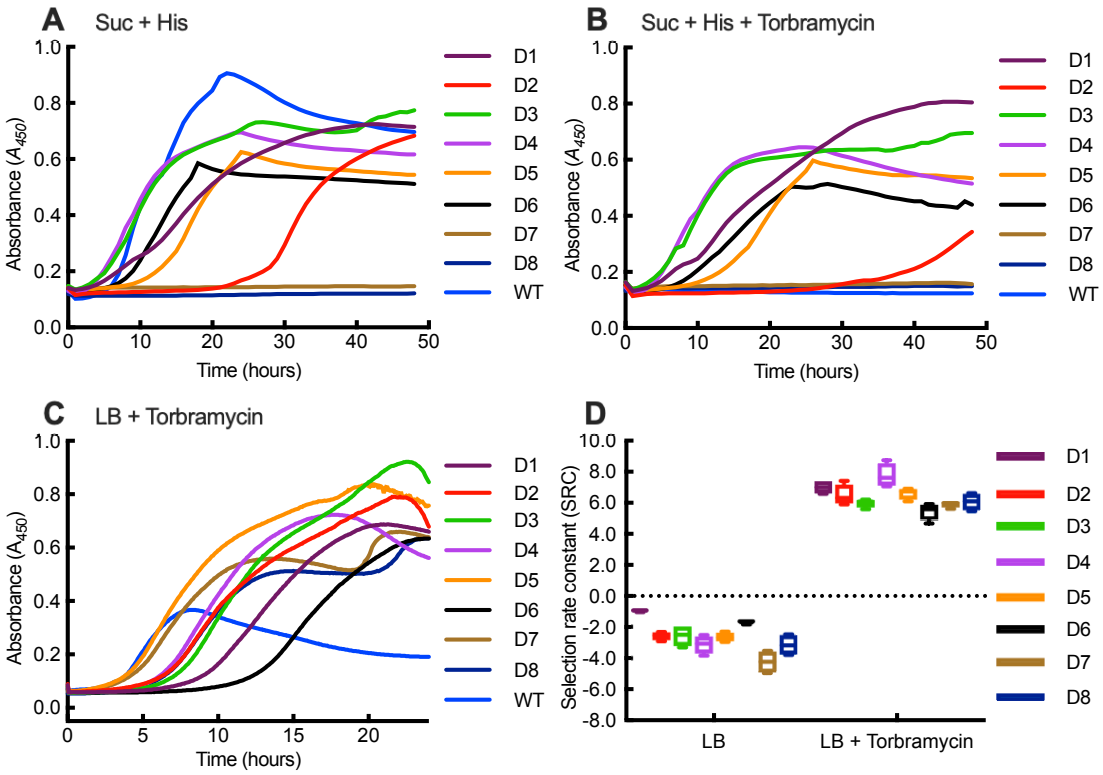

Figure 5. The Cu-evolved populations showed slower growth but an increase in tobramycin resistance.

(A) Growth dynamics in M9 salt medium supplemented with 20 mM succinate (Suc) and 10 mM histidine (His). **(B)** Growth in the same succinate and histidine medium with the addition of 2 µg/ml tobramycin. **(C)** Growth dynamics in LB containing 2 µg/ml tobramycin. Data are means of three independent cultures (errors bars are small and not shown for clarity). **(D)** Relative fitness of the bacterial populations to wild type in LB medium and LB with 2 µg/ml tobramycin. WT, wild-type *P. fluorescens* SBW25; D1 - D8, 320D1 to 320D8.

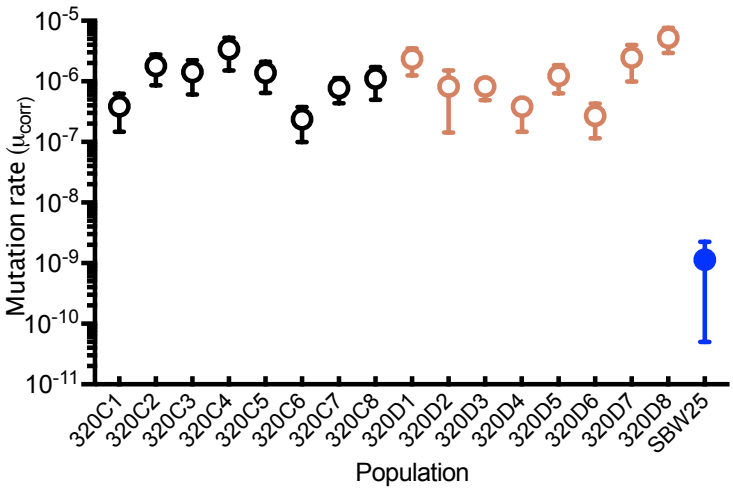

Figure S1. Mutation rates of the final evolved bacterial populations. Mutation rate per cell per division corrected by plating efficiency (μ_{corr}) was calculated using the bz-rates Web tool. A deletion mutation occurred in the eight control lines in the *mutS* gene: 254_GTC,AAG,CTG,GGC -> GGC; whereas a one "G" deletion occurred in a five "G" region of the *mutL* gene: 1174_(G)5 -> (G)4.

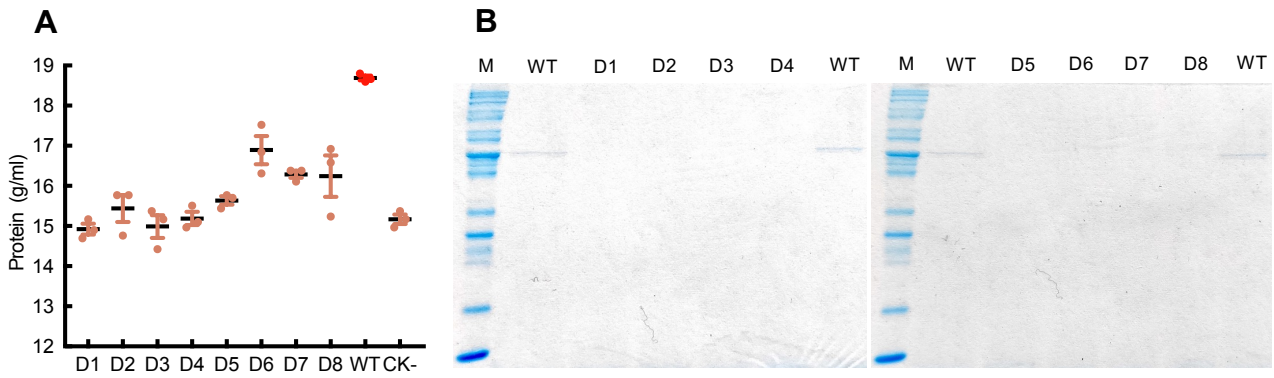

Figure S2. Analysis of exoproteins in the supernatants of copper-evolved populations grown in LB medium.

(A) Protein concentrations were determined using the standard Bradford assay. The black line in the middle represents the median of 3 independent cultures, whereas the lower and upper lines represent the 25th and 75th percentiles, respectively. One-way ANOVA multiple comparisons indicate significant differences ($P < 0.05$) with the wild-type (WT) control, except 320D6 and 320D8. **(B)** Images of two separate SDS-PAGE gels. Each well was loaded with 20 µl cell-free supernatants prepared from overnight cultures in LB broth. WT, wild-type *P. fluorescens* SBW25; D1 - D8, 320D1 to 320D8; CK-, LB broth without bacterial inoculation.

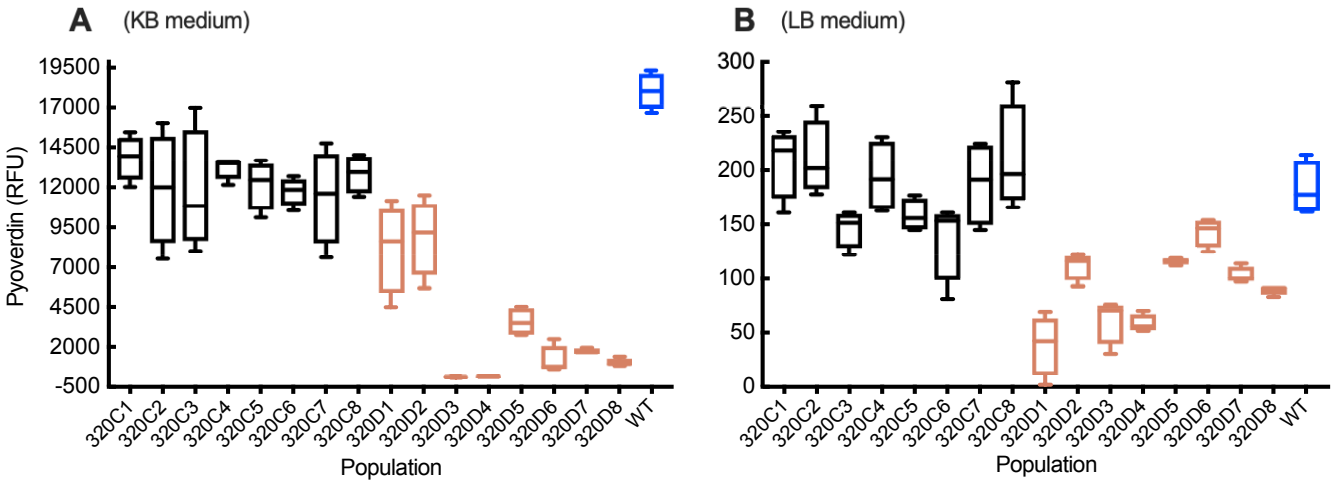

Figure S3. Decrease in pyoverdine production for bacteria grown in the laboratory media of KB (A) and LB (B).

Pyoverdine was quantified by measuring fluorescence of the culture supernatant at 460 nm and expressed as relative fluorescence units (RFU). The line in the middle of the box represents the median of 4 independent cultures, whereas the bottom and top boxes represent the 25th and 75th percentiles, respectively. The lower and upper whiskers indicate the smallest and largest values, respectively.